# INTELLIGENT ELECTRIC DRIVE SYSTEM
## *A mechatronics approach*

Guy Reginald Dunlop
*Department of Mechanical Engineering, Universityof Canterbury, PB4800, Christchurch, New Zealand*

Keywords: Mechatronics, Robotics, Intelligent drives, Model based control

Abstract: Drive efficiency is an important consideration in most robotic applications. A hybrid controller for permanent magnet DC motors has been developed to control the current, and hence the output torque of the motor. An H bridge is used to provide the basic PWM voltage to the motor, and the controller switches the bridge between bipolar and unipolar modes in order to minimise the switching losses within the bridge and motor, and also to minimise the electromagnetic interference. The first application presented is for a walking robot, and the second is for a dexterous robotic hand. In both cases, control is obtained from a voltage sourced inverter by means of a tight control loop that uses position readings to infer velocity so that a full DC motor model can be utilised in the control computer. For the dexterous hand, current control is by model prediction to avoid the need for direct measurement. The controller and communications are contained within a small programmable system on a chip which together with a dual H bridge driver is integrated into small circuit board that is used for distributed control within the hand.

## 1 INTRODUCTION

Most robots being manufactured are using permanent magnet electric drives, either DC or brushless DC. The ideas presented in this paper apply to both types of drive but discussion will be restricted to the brushed DC motor.

The walking machine *Hamlet* (Fielding and Dunlop, 2002) shown in fig. 1 utilises 18 electric motors. It has 6 legs each of which is operated by 3 DC motors. These can be clearly seen in the photograph. Each motor contains an integral shaft position encoder that provides position information for the kinematic calculations. The position information from a motor is also used to derive the velocity of the motor for use in the velocity servo loop contained inside the position feedback servo control loop. *Hamlet* was designed to explore the omnidirectional walking gaits of insects (Fielding and Dunlop, 2004) and as such it moves so slowly that regenerative energy issues need not be considered. The walker used 6 FPGA (field programmable array) units to control the 6 legs. The controllers communicated with off board DSPs via a single high speed serial bus and the control and kinematic decisions were computed on the DSPs. The H bridges were driven in bipolar mode (see section 2) and were robust enough to withstand brief current surges during speed reversals or changes.

Figure 1: The walking robot *Hamlet.*



Dunlop G. (2004).
INTELLIGENT ELECTRIC DRIVE SYSTEM - A mechatronics approach.
In *Proceedings of the First International Conference on Informatics in Control, Automation and Robotics*, pages 41-48
DOI: 10.5220/0001147900410048

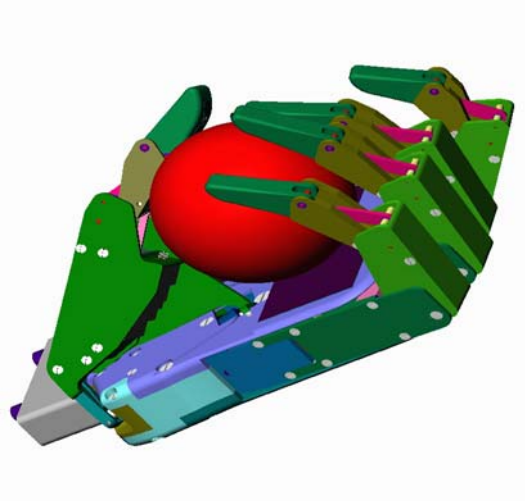

Figure 2: The dexterous Canterbury hand.

The miniature motors within the dexterous hand shown in fig. 2 are difficult to control as they have low inertia ironless rotors that have a low “thermal mass” and are easily overheated. A thermal model was needed to prevent this, and crucial to its operation, was precise control of the current in the motor to reduce resistive heating.

There are a total of 11 DC motors in the hand and 7 computers so temperature control is of some importance. As shown in fig.3, each finger contains 2 DC motors with a computer and driver unit. The heating of the motor armature during the current pulse needed to break joint stiction is transient, but the resulting temperature step is superimposed on top of the temperature within the hand. The need to minimise the temperature within the enclosed hand palm space lead to the development a very efficient drive system using a hybrid switching scheme for the DC motors. The various motor driving schemes are discussed in the next section followed by the application of models for current control which are presented along with simulation results.

## 2 BASIC DRIVE STRUCTURE

The purpose of any rotary actuator used in robotics is to produce torque and speed in a well controlled manner. This requires four quadrant control of the torque-speed characteristics of the driver and motor combination as shown in fig.5(a). No matter which kind of drive is used, none can handle situation where the load can drive the motor at a speed where the back emf is greater than the supply voltage unless additional overvoltage circuitry is added, something not required here.

Some commercial constant current IC drivers provide only two quadrant motor control and can be destroyed during regenerative operation when kinetic energy from the motor and robot is absorbed by the drive. The usual way to avoid this problem is to use a bipolar drive system that switches at ultrasonic frequencies so that four quadrant control is always achieved. However, the cost is more heat than for a unipolar drive system.

The H bridge driver shown in fig. 4 (4 FETs or field effect transistors form the left and right uprights and the motor the cross bar) requires only a single voltage supply. This is the most commonly used type of DC motor driver as it uses switching which is much more efficient than analog amplifier control. In operation, if FET 1 is on, then FET 3 is off, and vice versa. Similarly for FETs 2 and 4. The difference between unipolar and bipolar drive schemes has been discussed in detail by Tal, and Persson (1978) so only a brief outline is given here.

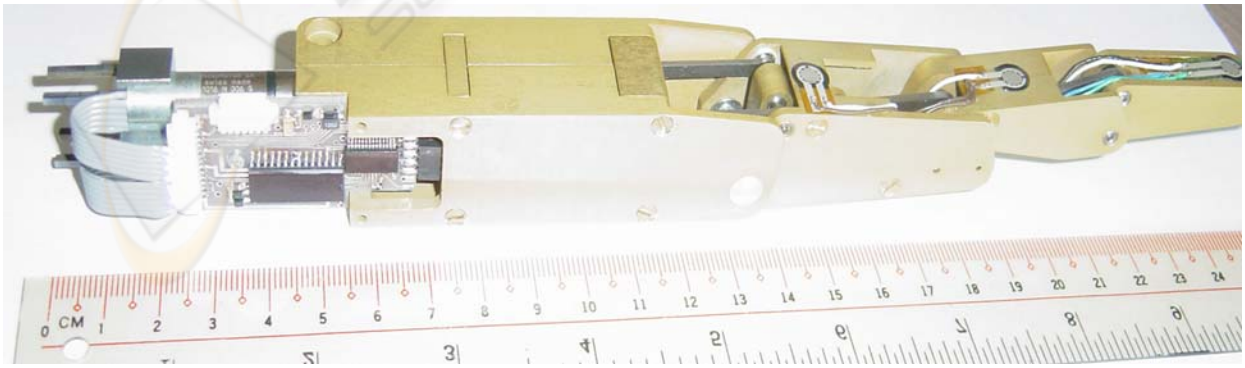

Figure 3: A finger from the hand showing the 2 DC motors and the control computer and driver PCB.

## 2.1 Bipolar Drives

When operated as a bipolar drive, both sides of the H bridge are switched on and off in antiphase with each other so that each end of the motor is connected alternately between zero volts and the supply voltage. The FETs act as switches for the current through the DC motor. FETs 1 and 2 are switched on for a time $\tau$ s every $T$ s, and then FETs 3 and 4 are on for the remaining ($T$ - $\tau$) s as shown in fig.5(b). The *PWM* (pulse width modulation) ratio is defined as $\tau/T$ and it is usual to chose $T < 50$ µs so that the switching is not audible. Neglecting the small voltage drops across the FETs and diodes (they are intrinsic to the FET), the governing equation for the average voltage across the motor is:

$$V_{av} = [\tau/T - 0.5]\, V_{supply} \qquad (1)$$

## 2.2 Unipolar Drives

The unipolar drive switches only one side of the H bridge. Referring to fig.4, the PWM signal is applied to FETs 1 and 3, while the sign of the average voltage applied to (and steady state current through) the motor is set by FET2. This halves the switching

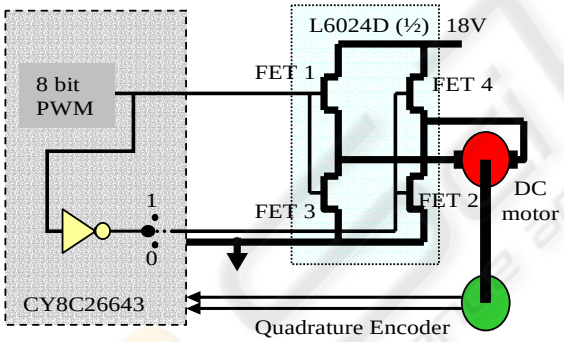


Figure 4: The control computer, the DC motor and encoder, and the H bridge (half an L6024D IC).

losses and heating is reduced. When operating at steady state with positive speed and torque (c.f. fig.5a), FET 2 is switched on (by setting logic 1 out) for a positive voltage applied to the motor. The voltage waveform is shown in fig.5(c).

The *PWM* signal is applied to FETs 1 and 3 so that the current through the motor increases whenever FET 1 is switched on, and decreases when ever FET 3 is on. The decaying current is able to circulate around the loop that includes the motor, and FETs 2 and 3. Only the back emf of the motor opposes the current and causes it to decay. The governing equation is:

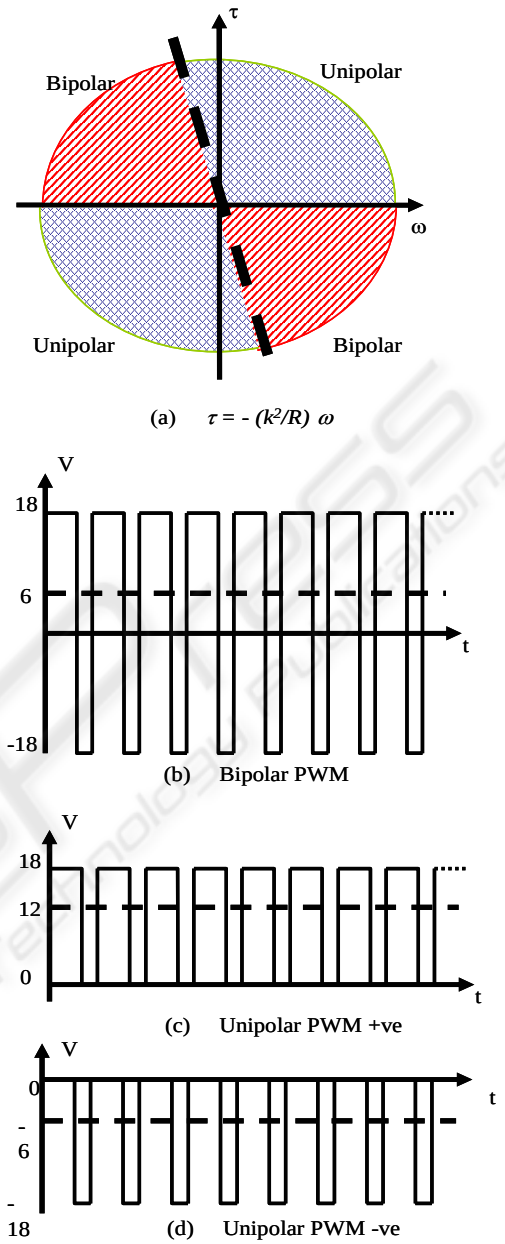


Figure 5: Four quadrant torque-speed plot. Motoring is in quadrants 1 and 3 of (a), and regenerative braking in quadrants 2 and 4. Efficient operation is obtained by using the unipolar PWM mode and switching to bipolar mode for the cross hatched regions in quadrants 2 and 4.

$$V_{av} = [\tau/T]\, V_{supply} \qquad (2)$$

To obtain a negative speed and torque, FET 4 is switched on by selecting logic 0. Switching FET 3 on then causes the magnitude of the negative current to increase with the negative voltage as shown in fig.5(d). Switching FET 1 on provides a path for

recirculation of the motor current through FETs 1

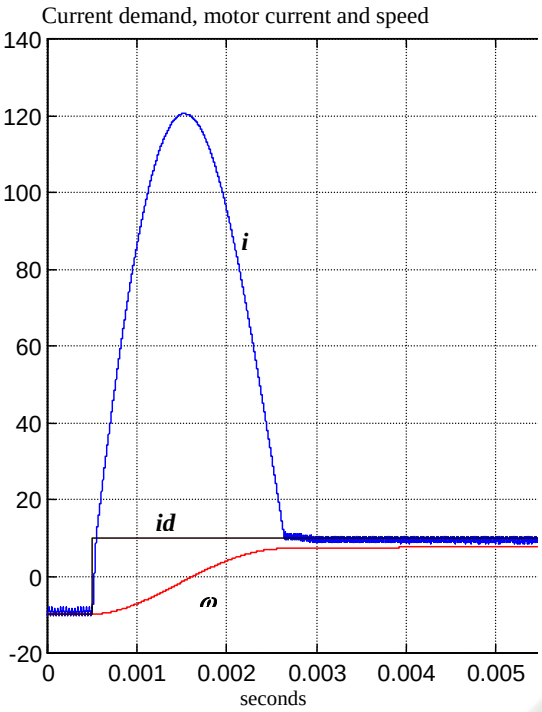


Figure 6: Over current during speed reversal with a unipolar drive and a large motor as id steps from -10A to +10A and ω changes slowly from -10 to +10

and 4. The governing equation is then:

$$V_{av} = [\tau/T-1]\, V_{supply} \quad (3)$$

The problems with unipolar drives arise when the motor speed needs to be reversed and the reversed current is established by a voltage reversal before the rotation direction has time to change. This happens (in quadrants 2 and 4) as the current magnitude increases when the supply is placed across the motor, but current still increases (at a slower rate) when recirculating as the back emf is now assisting the current. The result is a continual increase in the current until the motor slows and reverses. Currents of 40A have been measured (immediately before destruction) in a commercial IC rated for 3A in quadrants 1 and 3. The effect has been simulated for a large motor and the results presented in fig.6. The mechanism for this is found from the DC motor equations:

$$V_a = Ri + L\, di/dt + k\omega \quad (4)$$

$$\Gamma = ki \quad (5)$$

where $\omega$ is the motor speed in rads/s, $k\omega$ the back emf of the motor, and $\Gamma$ the torque output by the motor. When connected to the supply, the armature voltage $V_a = \pm V_{supply}$, and when recirculating the current, $V_a = 0$. Consider a change from negative speed to positive speed: In quadrant 3 the speed is still negative while the current has become positive, so when $V_a = 0$, the equation 4 becomes:

$$di/dt = -[k\omega + Ri]/L \quad (6)$$

Since ω is large and negative, the current magnitude will increase during the recirculate period until the back emf falls to the voltage drop across the resistance in the current recirculation loop. Equality occurs when $k\omega = -Ri$ or

$$\Gamma = -k^2\omega \quad (7)$$

This is shown as the dashed line in the 4 quadrant torque speed plot in fig.5(a).

## 3 HYBRID SWITCH CONTROL

The novel approach adopted Dunlop and Cree (1997) is to switch between bipolar and unipolar

Table 1: Drive switching scheme comparisons.

| Control Scheme | Avantages | Disadvantages |
|---|---|---|
| Bipolar | Good current control | Faster switching<br>More heat<br>More EMI |
| Unipolar | Slower switching<br>Less heat<br>Reduced EMI | No current control during regeneration |
| Hybrid | Good current control<br>Slower switching<br>Less heat<br>Reduced EMI | More complex circuitry |

control modes as required. The current through the motor is measured and used to switch from unipolar mode (cross hatched area in fig.5a) to bipolar mode when operation moves into the diagonally hatched area shown in quadrants 2 and 4 of fig.5(a). The detailed switching operation is illustrated in fig. 7 for a step change in demand current from -10A to +10A for the same large motor used for fig.6. Notice

that the current is fully controlled and that not much extra bipolar switching is required. The advantages and disadvantages of the 3 switching modes are listed in table 1.

The hardware used did not switch both sides at the same time so the negative voltage step changes were limited to $V_{supply}$ at any one time rather than $2V_{supply}$ for the bipolar drive. Software control can apply this to all bipolar drives and reduce electromagnetic interference from the drive.

The application of this hybrid switching technique to the hand precluded fast measurements of the motor current which changed very rapidly in the small motors that have low values of motor inductance *L* and relatively high resistance *R*. Such rapid current changes would require specialized hardware to track and control the current as was done by Dunlop and Cree. It would also need to operate an order of magnitude faster than for the larger motors tested with the hardware.

In order to reduce the hardware and heating requirements in the walker and hand, a model of the DC motor was used to calculate the motor voltage required for a given speed state and for the maximum torque available to change that speed. The maximum allowable current through the motor is used to achieve the speed change and that value must not be exceeded or excessive heating can destroy the motor. Software is then used to switch from unipolar driving to bipolar operation as the motor starts regenerating i.e. operating within diagonal hatched area in quadrants 2 and 4 in fig.5(a). As shown in fig.4, the output of the PWM is applied to FETs 1 and 3, while FETs 2 and 4 can be driven high or low to set the current direction for a unipolar drive depending on whether the signal is connected to logic 1 or 0 by software inside the CY8C6643 PSoC processor (programmable system on a chip c.f. Cypress Microsystems). When a bipolar drive is needed, the PWM is inverted and applied to FETs 2 and 4. Revision to a unipolar drive is simply a matter of by passing the inverted PWM signal and setting the processor output to 0 or 1 for FETs 2 and 4.

## 4 MODEL CONTROL

It is desirable to avoid using extra hardware for the direct measurement of the current in the motors. This lead to the development of model control for the 11 DC motors in the dexterous hand. A Simulink model of the DC motor used in the hand (a Minimotor 1016 012G) is shown in fig.8. The leadscrew driven linkages in the finger have a slight effect on the motor and gearbox, and almost none during regenerative braking as plain lead screws are not easily back drive. The main effect is the motor and gearbox inertia. The basic DC model includes the thermal power output by the armature resistance, and the effect of brush and bearing friction. This friction is overcome by the specified “no load” current but, as seen from equation 5, the no load current is zero. In fact the friction must be overcome and the “no load” current is required to do this. The friction is modeled as Coulomb friction which opposes the motion and decreases the torque

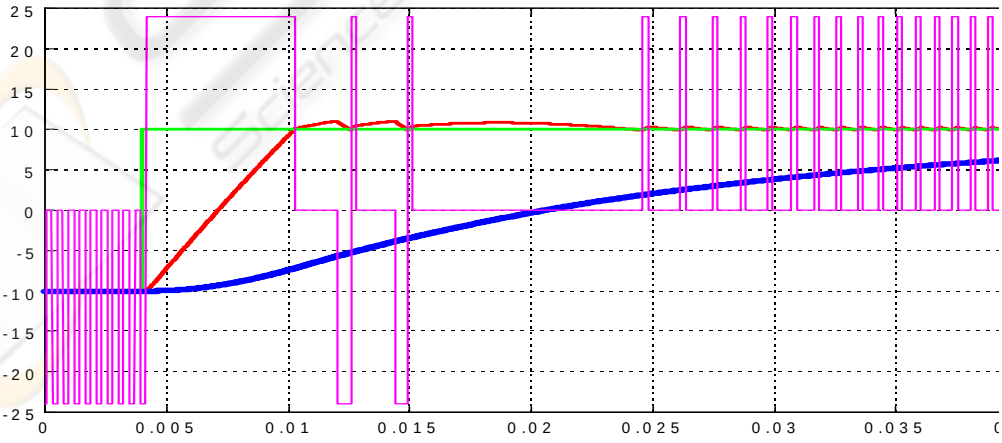


Figure 7: The rapidly switching line represents the motor drive voltage in response to the step reversal in current demand, the sloping line from -10A to +10A is the motor current, and the wide line from -10 to +10rads/s is the motor speed.

available for motoring in quadrants 1 and 3 of the torque-speed diagram shown in fig.5(a). The friction increases the braking during regenerative operation in quadrants 2 and 4.

test motor. The rate of change of the voltage applied to the DC motor is also limited to eliminate numerical problems associated with both the Simulink model, and in the PSoC controller which

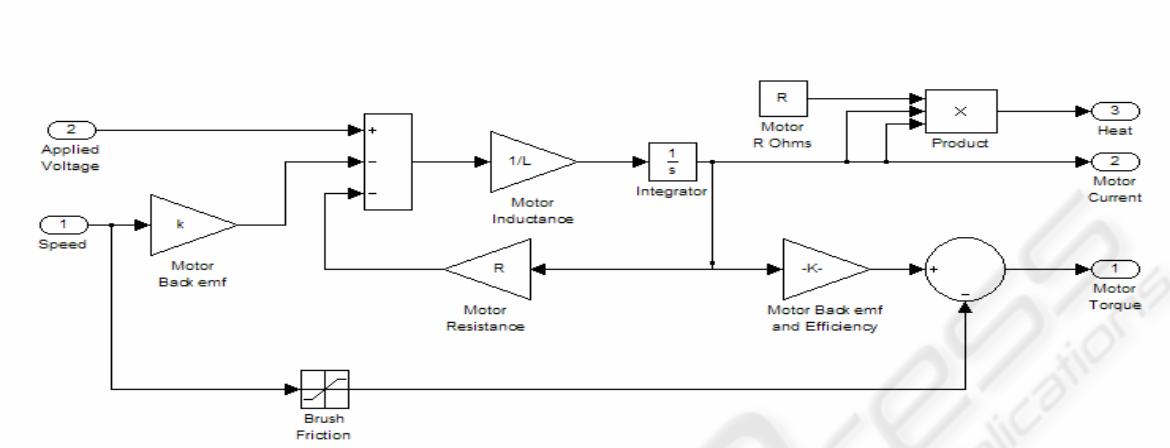


Figure 8: Simulink model of the Minimotor includes brush friction to account for no the load torque output.

When the voltage applied to the motor undergoes changes from +12V to -12V, the motor speed demand undergoes a step change from 1050 rads/s to -1050 rads/s as shown in fig.9, and the motor current peaks at 0.16A. The heating associated with these peaks during regeneration are a maximum of 2.8W and the average power is 0.38W for 0.1s reverse cycling. This is to be compared to the steady state running value of 0.26W. Thus an increase of 46% of heat in the motor must be dissipated which equates to a 46% rise in the temperature above ambient.

This model is placed inside a simple speed control loop as shown in fig.10. The voltage is limited to ±12V which is the supply voltage for the

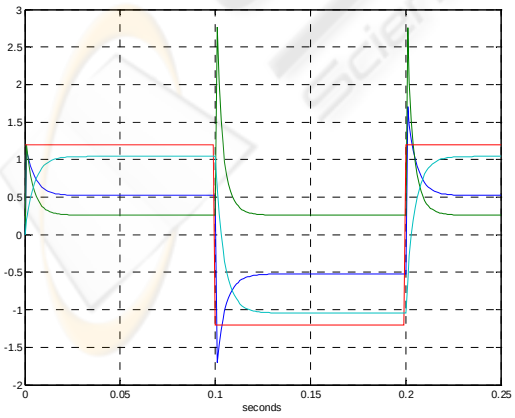


Figure 9: Responses of the control system and load to rectangular demands for speed change. From the top at 50 ms, the traces are: $V_a$ the average voltage applied to the motor (±12V), $\omega$ the motor speed in krads/s, $i$ the motor current (±50mA), and the heat produced in the armature windings in Watts.

converts the model voltage into PWM signals for the H bridge. The short term average of the H bridge output matches the voltage computed in the speed control loop. The performance for motor speed changes ±1000 rads/s is shown in fig.11(a). There are still large current peaks and the peak power is 2.8W with an average of 0.35W. Some improvement is needed.

Although this short speed reversing cycle is somewhat extreme, it does show the various factors that come into play. The main factor is to limit the voltage by a known amount relative to the back emf so that the current can be limited. Rather than applying a step of voltage to the motor, the voltage can be changed slowly to match the speed changes.

The Simulink model shown in fig.12 contains a sub loop to control the voltage demand. This is simply a model of the electrical part of the motor with no provision for friction. The derivative of the shaft position output from the gearbox is used to derive the speed, and after adjustment for the gearbox ration, this speed estimate is used in the velocity feedback loop as well as in the DC motor model that is used to estimate the motor current that would result from the application of the voltage output by the speed error to voltage block in fig.12 (shown as gain and limit blocks in fig.10). The friction does not need to be modeled in the current estimator; it is effectively taken care of since the measured position and derived speed are already reduced by the friction. The dead zone for the current limit, gain and summation junction that

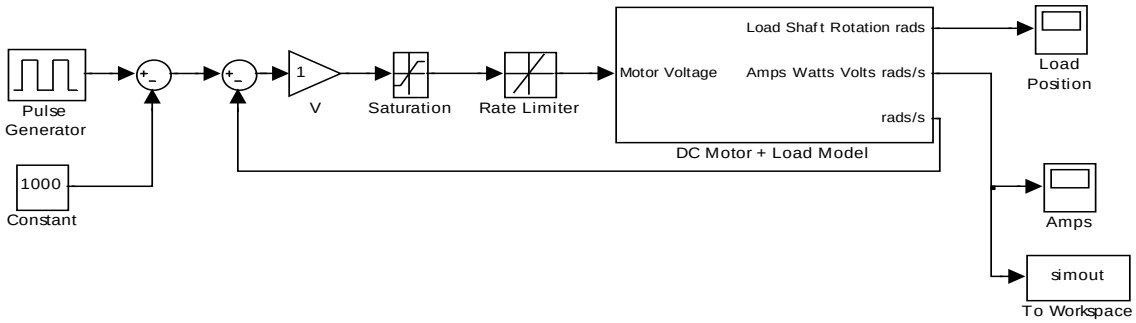


Figure 10: A finger from the hand showing the 2 DC motors and the control computer and driver PCB.

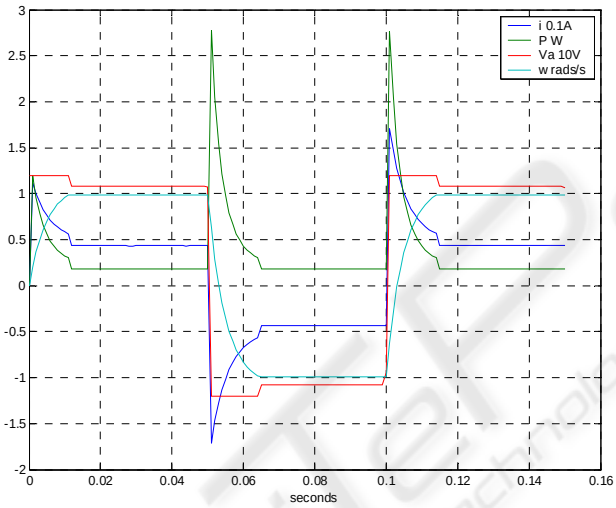


Figure 11: Speed demand is 0 →+1000→-1000→+1000 rads/s. The drive saturates at ±12V. The peak and average power dissipation is 3.5W, average of 0.35W using the controller in fig.10. The peak current is 0.17A

follow the estimator are used to decrease the voltage if excessive motor current would result from directly applying the demand voltage.

## 5 DISCUSSION

The use of a velocity control loop within a position control loop ensures that good positioning performance can be attained. Hower, large speed demands translate into large voltages being applied to the DC motor, and this can give rise to large currents, and excessive heating. The use of a current estimator that has the voltage demand and the actual motor speed as inputs has been shown to provide good estimates of the current that would occur should the demand voltage be placed on the actual motor and load. A dead zone is used to process the estimated current so that no output occurs unless the specified motor current limits are exceeded (note that the limits used here are for inside the hand, not those specified by Minimotor for a motor with free air circulation). When the estimated current exceeds the limits set, then the excess current value is converted to a voltage that is subtracted from the demand voltage to give a modified voltage for application to the actual motor.

## 6 CONCLUSION

The novel approach used here has proved adequate for control of the heat build up within a confined space when several motors are used. Control of the motor current was crucial for this and as demonstrated, good control was obtained by using a model current estimator implemented on a small control microprocessor. The processor also allowed for a hybrid switch control of the H bridge to be used to further reduced the heating. The PSoC

controller converts this modified voltage to a PWM value. It also takes into account the sign of the voltage and the direction of rotation so that the appropriate PWM mode can be selected.

## REFERENCES


Tal, J., and Persson, E.K., 1978. Pulsewidth modulated amplifier for DC servo systems. *Proc. 7th Symp. on Incremental Motion Control Systems and Devices: DC motors and control systems*, Eds. B.C.Kuo, and J.Tal, SRL Publishing Co., ISBN 0-918152-02-X, Vol. 1, ch.11, pp180-200.

Fielding, M. R., and Dunlop, G. R., 2002. Omni directional hexapod walking and efficient gaits using restrictedness, *Proc 5th Int. Conf. on Clinbing and Walking Robots.* ISBN 1-8600-5838-06, pp 501-508.

Fielding, M. R., and Dunlop, G. R., 2004. Omni directional hexapod walking and efficient gaits using restrictedness. *Accepted for IJRR.*

Dunlop, G. R., and Cree, A., 1997. A four quadrant current driver for direct digital control of a DC motor. *Proc. 26th Symp. on Incremental Motion Control Systems and Devices*, Ed B.C.Kuo, SRL Publishing Co., ISBN 0-931538-20-3, pp 143-150.

Cypress Microsystems *www.cypressmicro.com*


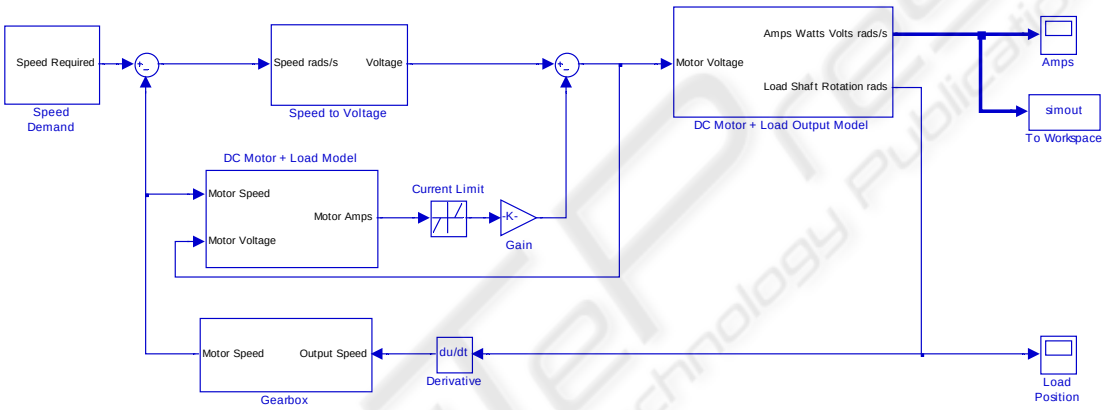


Figure 12: A finger from the hand showing the 2 DC motors and the control computer and driver PCB.

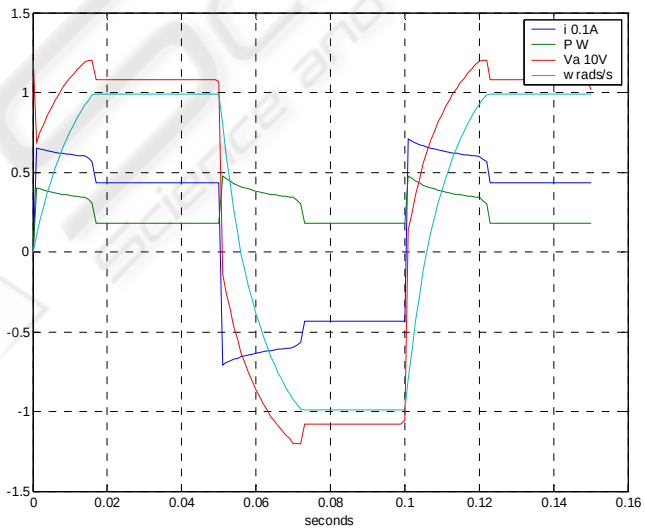


Figure 13: Speed demand is 0 →+1000→-1000→+1000 rads/s. The voltage drive saturates at ±12V. The peak e power dissipation is 0.45W with an average of 0.25W for the controller in fig.12. The peak current is around 0.07A so current control is greatly enhanced.